Journal of Computer Assisted Tomography
10(1):1–9, January/February

MR Imaging of the Lung Using Liquid Perfluorocarbons

Stephen R. Thomas, Leland C. Clark, Jr., Jerome L. Ackerman, Ronald G. Pratt, Richard E. Hoffmann, Lawrence J. Busse, Robert A. Kinsey, and R. C. Samaratunga

Abstract: Certain perfluorocarbon (PFC) compounds, commonly used as the oxygen transport components of "blood substitutes," may be breathed as neat liquids with survival because of their chemical inertness and their high solubility for oxygen and carbon dioxide. In addition, the paramagnetism of oxygen reduces the fluorine T1 value according to an inverse relationship allowing a potential method of monitoring Po_2 gradients in vivo. This article presents the results of magnetic resonance (MR) imaging of the lungs of mice and rats following breathing of four PFC liquids (FC-43, FC-75, PFOB, APF-215). The images presented were obtained at two magnetic field strengths (0.66 and 0.14 T) under conditions of breathing either ambient air or pure oxygen. Spin-lattice relaxation times (T1) for the PFCs are measured both in vitro and in vivo (in the lungs) as a function of the state of oxygenation. A MR image signal strength enhancement of up to 90% is demonstrated in vivo under conditions of pure oxygen breathing. **Index Terms:** Fluorine—Contrast media, inhalation agents—Magnetic resonance imaging.

In 1966 the demonstration by Clark and Gollan (1) that certain perfluorocarbon liquids could be breathed with survival initiated the use of highly fluorinated organic compounds for respiration and artificial blood. The suitability of perfluorocarbons for these applications was based on the properties of chemical and biological inertness combined with the ability to dissolve up to 60 volume % of oxygen and 120 volume % of CO_2 (2). Initial research focused on the oxygen and carbon dioxide transport capability in an effort to identify fluorocarbons with the best molecular structure to form emulsions for intravascular use while confining body retention to the period of functional usefulness (3). Emulsions of the perfluorocarbon compounds (PFCs) are beginning to show increased utility in biological and clinical applications (4–6). The potential of ^{19}F magnetic resonance (MR) imaging (7–9) has opened significant new avenues for highly sensitive investigations of the in vivo properties and diagnostic capabilities of the PFCs. Recent investigations have shown the feasibility of MR imaging of PFC emulsions and neat liquids (10–12). Some of these studies have demonstrated the potential for in vivo oxygen "imaging" in blood and organ tissue through the paramagnetic effect of dissolved oxygen, which reduces the PFC T1 value (10,11,13) and lung ventilation imaging following liquid breathing of the PFC (14). An expanded new range of possibilities may be envisioned for the medical use of PFCs including diagnostic procedures that allow biomedical monitoring of organ function, the study of biochemical mechanisms in vivo, and the development of therapeutic techniques. This article will report on the techniques, current results, and future expectations for MR imaging of the pulmonary system using liquid breathing of PFC neat liquids.

From the Department of Radiology, College of Medicine, University of Cincinnati (S. R. Thomas, R. G. Pratt, L. J. Busse, and R. C. Samaratunga), Children's Hospital Research Foundation (L. C. Clark, Jr., and R. E. Hoffmann), Department of Chemistry, University of Cincinnati (J. L. Ackerman), and Miami Valley Research Laboratories, Procter and Gamble (R. A. Kinsey), Cincinnati, OH. Address correspondence and reprint requests to Dr. S. R. Thomas at University of Cincinnati, College of Medicine, E465 Medical Science Building, Mail Location No. 579, Cincinnati, OH 45267, U.S.A.

Characteristics of ^{19}F Relevant to MR Imaging Studies and the General Properties of PFCs

The characteristics of ^{19}F that make this nucleus uniquely suited for high contrast MR imaging in vivo are well recognized; namely, a high magnetogyric ratio (40.05 MHz/T), spin ½, a sensitivity rel-

TABLE 1. *Properties of the four perfluorocarbon compounds used in this study*

Name and code[a]	Chemical formula	Density (g/ml) 25°C	Vapor pressure (mm Hg) 37.5°C	Viscosity (cs)[b] 25°C	Surface tension (dynes/cm) 25°C	Oxygen solubility (ml/100 ml) 25°C
F-butylfuran:						
FC-75 (or FC-80)	$C_8F_{16}O$	1.78	51	0.82	14.8	52.2
F-octyl bromide:						
PFOB	$CF_3(CF_2)_7Br$	1.89	15	1.0	16.4	52.7
F-tributylamine:						
FC-43 (or FC-47)	$(CF_3CF_2CF_2CF_2)_3N$	1.90	2.5	2.52	16	38.4
F-Phenanthrene:						
APF-215	$C_{14}F_{24}$	2.02	0.3	8.03	—	35

From ref. 2.

[a] FC-43 (FC-47) is a mixture of isomers of perfluorotributylamine. FC-75 (FC-80) is a mixture of isomers of perfluorobutyltetrahydrofuran. Both of these are obtained from the 3M Company. PFOB is perfluoro-octylbromide, a gift from Dr. David Long. APF-215 is a mixture of isomers of perfluorophenanthrene, purchased from PCR, Florida. "F-" is a prefix that indicates "perfluoro."

[b] The centistoke (cs) is a unit of kinematic viscosity defined as 10^{-2} times the viscosity divided by the density ($0.01\eta/\rho$). A viscosity $\eta = 1$ dyne · s · cm^{-2} is called a poise.

ative to protons of 0.83, 100% natural isotopic abundance, and an extremely low intrinsic biological occurrence. Aspects relating the total body occurrence in man to ^{19}F tracer MR imaging have been discussed (9) and indicate that, under the conservative assumption that 2.6 g of fluorine is uniformly distributed throughout the body of a 70 kg man, the intrinsic concentration would be ~1.9 m*M*. However, the actual soft tissue concentration is less because much of the ^{19}F is likely to be incorporated into bone mineral (for example as fluoroapatite). Any resonance arising from such motionally hindered ^{19}F will be broadened and/or have so long a longitudinal relaxation time as to be unsuitable for an imaging experiment.

The following list provides a summary of the properties desirable for a PFC if it is to be considered as a candidate for use in liquid breathing followed by in vivo MR lung imaging: (a) low viscosity (at a value of water or less) that is required to ensure that the normal lung mechanics associated with breathing will be sufficient to provide physical transport of the liquid into the small alveolar spaces; (b) high vapor pressure to provide an acceptably limited retention time within the lung; (c) nontoxic; and (d) a large number of equivalent fluorine atoms/unit volume to provide, ideally, a single dominant spectral line representing the optimal condition for MR imaging. In relation to this fourth point, as will be discussed below, the PFCs in fact have complicated MR spectra resulting from the nonequivalent chemical environments for the individual fluorine atoms within the molecular configuration. This characteristic gives rise to complications, including degradation of signal-to-noise (S/N) performance and chemical shift artifacts, which must be addressed in the MR imaging phase.

The research to be reported in this article has involved four perfluorinated liquids: F-butylfuran (FC-75 or FC-80), F-octylbromide (PFOB), F-tributylamine (FC-43 or FC-47), and F-phenanthrene (APF-215). The prefix "F-" is used as shorthand for "perfluoro." It should be noted that the names "propylfuran" and "phenanthrene" are not chemically correct but rather labels that have been used in the industry. The compounds are in fact saturated perfluoroalkanes and are supplied as mixtures of isomers. Names that would be more chemically correct are "F-propyltetrahydrofuran" and "F-perhydrophenanthrene," respectively. Table 1 reviews the relevant general properties of these compounds. F-octylbromide is radiopaque as a result of the single bromine atom incorporated at the end of the CF-chain. Thus, this fluorocarbon has the unique capability of allowing radiographic correlation of the PFC distribution with the corresponding MR image. The MR multiline spectra of these four compounds are shown in Fig. 1.

In an attempt to understand the physicochemical basis for the high solubility of oxygen in PFC liquids

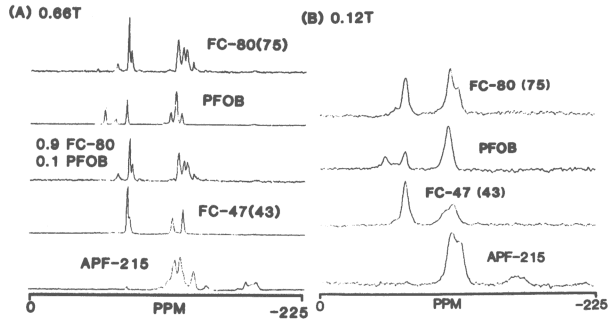

FIG. 1. The chemical shift spectra of the perfluorocarbon compounds used in this research. **a:** Magnetic field strength 0.66 T, 26.4 MHz for ^{19}F. Taken on the high field, small geometry MR system described in the text. **b:** Magnetic field strength 0.12 T, 4.8 MHz for ^{19}F. Taken on the whole body, resistive MR system described in the text.

(2) a number of investigations have been reported (15–18). They all show that there is no preference of oxygen for a particular site. The potential for the in vivo MR imaging of oxygen tension (Po_2) in tissue and organs using the PFC compounds has been demonstrated in earlier studies (10,11,14). This possibility is based on the intrinsic paramagnetic property of O_2, which significantly affects the spin-lattice relaxation time, T1, of the PFC. The spin-lattice relaxation rate $(T1)^{-1}$ has been found to increase linearly with Po_2 (10,11,13,17,19). Thus, with the proper selection of the pulse protocol sequence, regions of higher Po_2 may be enhanced in the PFC MR image. Ultimately, analysis of calibrated T1 images may be envisioned to provide in vivo Po_2 mapping.

The observed spin-lattice relaxation rate $T1^{-1}(obs)$ of a single resonance line is given by $T1^{-1}(obs) = T1^{-1}(int) + T1^{-1}(Po_2)$. The quantity $T1^{-1}(int)$ is the intrinsic relaxation rate due to all mechanisms not involving relaxation via the dipolar coupling to the unpaired electron spin density of the oxygen molecule in solution. The quantity $T1^{-1}(Po_2)$ is a term that is proportional to the number of oxygen molecules per unit volume of the fluorocarbon phase, which in turn is proportional to the Po_2 of the environment surrounding the fluorocarbon phase. This latter proportionality is due to the reasonably ideal Henry's law solubility characteristics of O_2 gas in PFCs. The value of the proportionality constant relating Po_2 and $T1^{-1}(Po_2)$ depends on the particular PFC, the resonance line measured, and the temperature (which affects both the motional correlation time for the ^{19}F-electron dipolar interaction and the O_2 gas solubility). In principle, it can also depend on the magnetic field strength (which could alter the electron T1 to a value where this T1 dominates the motional correlation time), although this is not observed at our field strengths.

MATERIALS AND METHODS

Two MR imaging systems were involved in this work. Both systems were designed and developed at the University of Cincinnati. The first system, described in detail elsewhere (9), is a small geometry, 1.45 T unit based around a Varian Associates (Palo Alto, CA, U.S.A.) 4013A iron core resistive electromagnet. It has 12 inch diameter pole faces with an intrinsic 2.25 inch (5.7 cm) separation. However, the final sample access is only ~2.1 cm in diameter as a result of the constraints imposed by the original shim coils (used to provide the gradient fields), flux stabilizer coils, and the radiofrequency (RF) probe housing. Thus, this system is limited to investigations involving phantoms, small perfused organs, and small animals (20 g mice). The in vivo imaging experiments on mice were conducted in the range of 0.6–0.7 T (25–28 MHz for fluorine), which represents approximately one-half the maximum field strength of the magnet.

The second system capable of whole body MR imaging is based around an Oxford Instruments Limited (Oxford, England) 0.15 T six-coil air core resistive magnet (20). The clear bore diameter is 80 cm. However, access is limited to the 20 inch (51 cm) inner diameter of the current gradient coils. The rat imaging results described below used a 10 cm inner diameter solenoidal RF coil in a horizontal orientation perpendicular to the primary magnetic field. The same spectrometer console was used for both magnet systems.

The liquid breathing procedure involves immersing the awake animal in the oxygen-bubbled fluorocarbon liquid for a time sufficient to fill the lungs (several minutes). The PFC properties of high O_2 solubility and inertness allow the animals to breathe while submerged without any detrimental effects. Figure 2 illustrates the apparatus used for mice. The advantage of this particular design is that it allows the use of less total volume of the given fluorocarbon than would be required by a standard immersion beaker while at the same time comfortably restraining the animal. Currently, because of their larger size, the rats have been held gently by hand and immersed in a 4 L beaker containing the oxygen-bubbled PFC.

Following the liquid breathing, the animals are removed from the PFC environment and inverted

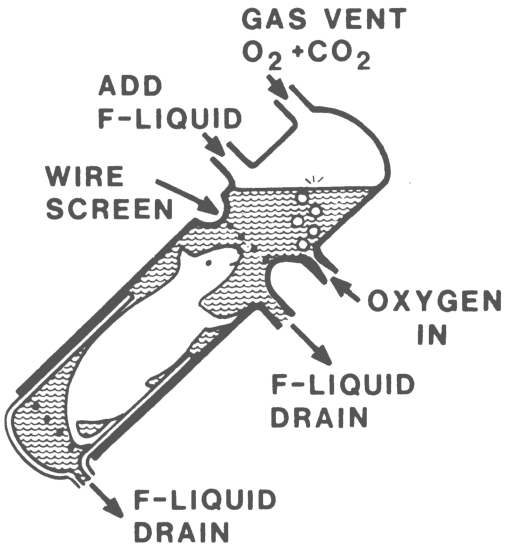

FIG. 2. A schematic of the apparatus used for the liquid breathing of mice. This design allows a limited volume of perfluorocarbon compound to be used while comfortably restraining the animal.

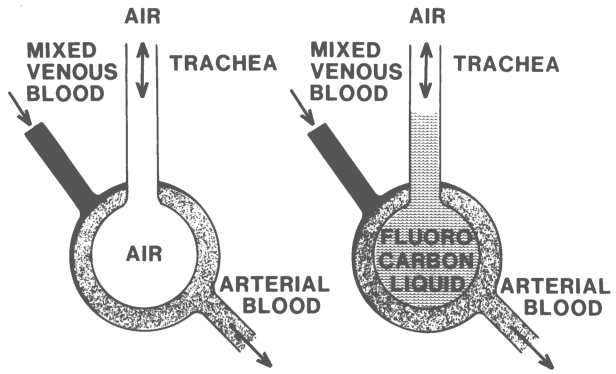

FIG. 3. A schematic illustrating the phenomena of residual perfluorocarbon liquid trapped within the alveolar space following liquid breathing and attempted draining. The MR lung imaging is performed on this residual PFC with the animal breathing ambient air or pure oxygen. Efficient oxygen transport through the PFC volume represents a characteristic property of these materials.

(head down) to drain the fluorocarbon liquid from the body and lungs. They are rinsed with a high vapor pressure PFC (FC-75) as an aid to drying their fur. The animals are then placed in a pure oxygen environment until they are completely dry and it becomes obvious that they can support their own respiration. The ^{19}F MR imaging of the lungs with the animal breathing ambient air or pure oxygen is based on the residual fluorocarbon, which has been retained (trapped) within the alveolar spaces. Figure 3 provides a schematic representation of this concept.

The animals involved in this investigation were 20 g Swiss albino (young adult) mice and Sprague-Dawley rats. In preparation for the MR studies the mice and rats, which have been fasted for 12–24 h, receive an intraperitoneal injection of sodium pentobarbital, 60 and 40 mg/kg, respectively. This is sufficient to provide anesthesia for 1–2 h, thus allowing ample time for a series of imaging experiments.

The MR imaging of the PFCs in vivo is complicated on two levels: (a) The quantity of the PFC introduced into the body is limited, resulting in relatively low S/N conditions. When used intravascularly, as an emulsion, the PFCs are further diluted from the neat liquid to 10 or 20% by volume; (b) the PFC ^{19}F spectra as shown in Fig. 1 exhibit multiple lines (due to chemical shifts and indirect spin-spin couplings) of varying frequency spacing and intensity. These characteristic spectra present a challenge for MR imaging in that they represent a nontrivial system response function that must be accounted for in the reconstruction process (distinct from the single spectral line given, for example, by the proton of water). The distribution of the ^{19}F signal intensity over multiple lines decreases the S/N characteristics compared to the S/N that would be obtainable from a single line spectrum, introduces artifacts through chemical shift "ghost" images, and degrades the spatial resolution. Aspects of our research, as reported elsewhere (21), have concentrated on developing methods for improving the S/N in PFC MR imaging through application of computer processing techniques involving: (a) projection windowing algorithms to remove selected chemical shift lines; (b) deconvolution methods incorporating the complex spectral line pattern as a corrective system response function; and (c) application of multiplexing techniques that fold in the signal from spectrally isolated lines or groups of lines. Some of these methods, which will not be described in technical detail in this paper, have been applied in the reconstructed images to be shown below.

To increase the received S/N ratio, the technique of "shadow imaging" or "projective imaging" was used, which refers to the nontomographic, conventional X-ray film presentation in which the three-dimensional object is projected onto a two-dimensional plane. The equivalent of this type of image may be obtained in MR imaging by using a nonselective excitation RF pulse/gradient protocol that does not provide any narrow slice definition. Thus, if the image plane of interest is chosen to be the transverse (axial), with G_y and G_z serving as the readout gradient components, $G_x = 0$, and use of nonselective RF pulses (i.e., no slice selection), the resultant image produced by filtered backprojection reconstruction techniques represents the projection of the region of fluorine concentration onto the y–z plane. Similarly, a coronal plane projection image may be obtained using G_x and G_z as the readout gradients with $G_y = 0$. These concepts are illustrated in Fig. 4.

RESULTS AND DISCUSSION

Table 2 provides results of both the in vitro and in vivo T1 measurements that were made on the various PFCs. For FC-75 and PFOB, relatively large changes in T1 are observed in vitro when going from a Po_2 near zero (nitrogen bubbled) to a highly oxygenated state (oxygen bubbled). A smaller decrease in T1 over this same range of Po_2 values is evident for FC-43 and APF-215. To achieve a sensitive differentiation between regions of differing Po_2, it is desirable that the lowest and highest oxygenation states span a wide range of T1 values. Of particular interest in the PFC lung imaging investigations is the change in T1 when breathing pure oxygen versus ambient air. The smallest differential effect on T1 was observed for APF-215. The in vivo lung values obtained for FC-43 and the FC-75/PFOB mixture show a decrease

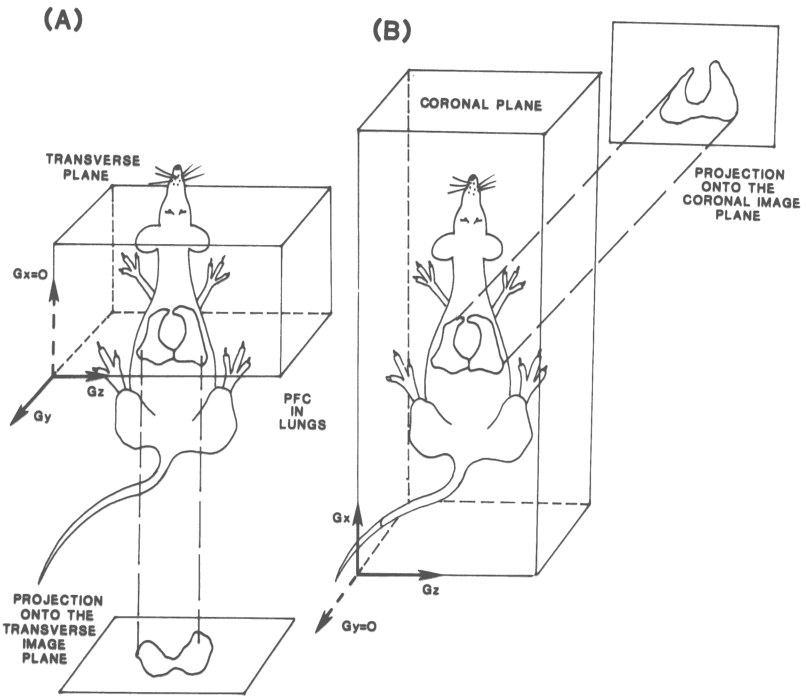

FIG. 4. A schematic illustrating the production of "shadow" images. The technique involves nonslice selective pulse protocols with the *x*-gradient equal to zero for the transverse image plane projection **(a)** and the *y*-gradient equal to zero for the coronal projection **(b).**

TABLE 2. *Relaxation parameters as a function of Po_2 for the various neat liquid perfluorocarbon compounds (PFC)*

PFC	Condition	Bo (T)	MHz	$(T1)^{-1}$ (s^{-1})	T1 (ms)
FC-43	In vitro				
	1. Oxygen bubbled	a. 0.14	5.7	6.67	150 ± 30
		b. 0.66	26.5	5.21	192 ± 30
	2. Air bubbled	a. 0.14	5.7	2.50	400 ± 50
		b. 0.66	26.5	2.09	479 ± 50
	3. Nitrogen bubbled (Po_2 = 0)	a. 0.14	5.7	1.61	620 ± 50
		b. 0.66	26.5	1.32	759 ± 70
	In vivo: whole lung (mouse)				
	1. Air breathing	0.66	26.5	1.49	670 ± 50
	2. Oxygen breathing	0.66	26.5	3.70	270 ± 50
FC-75	In vitro				
	1. Oxygen bubbled	a. 0.14	5.7	5.26	190 ± 30
		b. 0.66	26.5	3.70	270 ± 30
	2. Air bubbled	a. 0.14	5.7	1.85	540 ± 100
		b. 0.66	26.5	0.89	1,120 ± 110
	3. Nitrogen bubbled (Po_2 = 0)	a. 0.14	5.7	0.25	4,040 ± 500
		b. 0.66	26.5	0.23	4,270 ± 400
PFOB	In vitro				
	1. Oxygen bubbled	a. 0.14	5.7	5.56	180 ± 30
		b. 0.66	26.5	3.70	270 ± 30
	2. Air bubbled	a. 0.14	5.7	1.27	790 ± 50
		b. 0.66	26.5	1.08	929 ± 90
	3. Nitrogen bubbled (Po_2 = 0)	a. 0.14	5.7	0.42	2,390 ± 500
		b. 0.66	26.5	0.42	2,390 ± 20
90% FC-75	Ambient air				
10% PFOB	In vitro	0.66	26.5	1.39	720 ± 50
90% FC-75	In vivo: whole				
10% PFOB	lung (mouse)				
	1. Air breathing	0.66	26.5	0.89	1,120 ± 100
	2. Oxygen breathing	0.66	26.5	2.0	500 ± 100
APF-215	In vitro				
	1. Oxygen bubbled	a. 0.14	5.7	10.00	100 ± 30
		b. 0.66	26.5	5.99	167 ± 20
	2. Air bubbled	a. 0.14	5.7	3.45	290 ± 50
		b. 0.66	26.5	3.33	300 ± 30
	3. Nitrogen bubbled (Po_2 = 0)	a. 0.14	5.7	2.48	410 ± 40
		b. 0.66	26.5	2.48	404 ± 40

in T1 of ~400 and 600 ms, respectively, at 0.66 T when changing from ambient air breathing to pure oxygen. The in vitro results at 0.14 T for the air bubbled and oxygen bubbled states show a change in T1 value of 250, 360, and 610 ms for FC-43, FC-75, and PFOB, respectively. For APF-215 a comparison of the in vitro results at 0.14 T shown in Table 2 for the air versus oxygen bubbled states indicates that a somewhat smaller decrease in T1 of ~180 ms was obtained. Thus, APF-215 is not the optimal candidate for use as a differential oxygen tension monitor because its T1 sensitivity to differences in P_{O_2} is limited.

A schematic representation of the white rat heart/lung geometry as modified from ref. 22 is shown in Fig. 5. The left side consists of a single lobe whereas the right is more complex, consisting of multiple lobes. The heart (which will provide a null signal demarcation in the ^{19}F MR image) is located near midline with the major axis close to vertical (or with the apex tipped slightly to the left). The heart/lung anatomy for the mouse exhibits similar geometry on a smaller scale.

Figure 6 presents the posteroanterior radiograph and the transverse MR lung field images of a mouse following liquid breathing of a 2-to-1 FC-75/PFOB mixture. Specific details of the MR pulse protocol and reconstruction methods are given in the caption. As seen in the radiograph, some of the PFC mixture was swallowed and may be visualized in the stomach and intestines. As an adjunct to the primary lung imaging investigation, this figure and the next two illustrate the potential of using perfluorocarbons as gastrointestinal contrast agents. The transverse MR images indicate that the left lung field is somewhat smaller than the right, which correlates with the radiographic appearance showing the heart shadow slightly off midline toward the left. The MR image taken while the animal was breathing pure oxygen was enhanced in signal strength by approximately 10% over that taken while breathing ambient air. The relatively short recycle delay time (TR) of 150 ms allowed discrimination through the reduction in T1 which, as stated previously, is decreased by the paramagnetic effect of the oxygen. For the two oxygenation states, the lung fields appear geometrically similar; however, the enhanced image improves definition of the peripheral extent of the lungs. Whole body transpiration data for the first several days following the MR imaging showed that the animal exhaled ~1 and 4 μl/day of FC-75 and PFOB, respectively.

The radiographic and MR images of another mouse following liquid breathing of the 2-to-1 FC-75/PFOB mixture are shown in Fig. 7. Prior to the liquid breathing a defect was surgically introduced into the left lung involving acute obstruction of a bronchial branch. This particular mouse died shortly before the MR experiments began; conse-

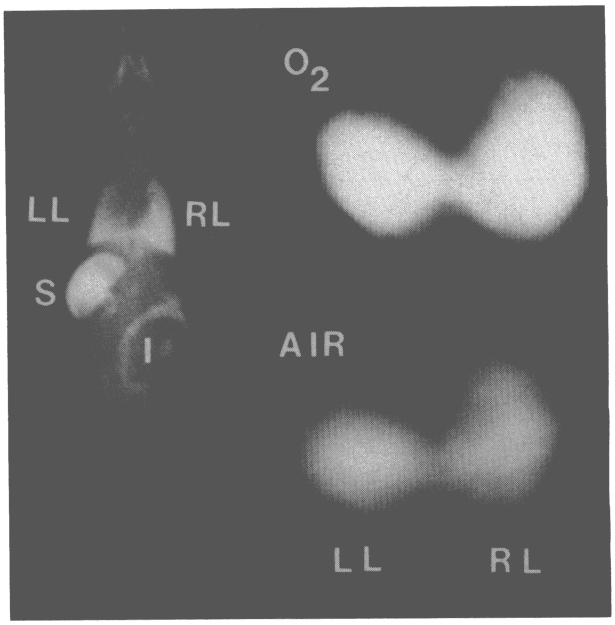

FIG. 6. Radiograph (posteroanterior) **(left)** and transverse MR images **(right)** following liquid breathing of a 2-to-1 FC-75/PFOB mixture. The signal strength enhancement as a result of pure oxygen breathing is evident. Abbreviations: intestines, I; left lung, LL; right lung, RL; stomach, S. MR technique: 25.1 MHz (~0.63 T for fluorine); partial saturation, 150 ms recycle delay (TR); 128 averages/projection; 72 projections; gradient strength 0.09 G/cm.

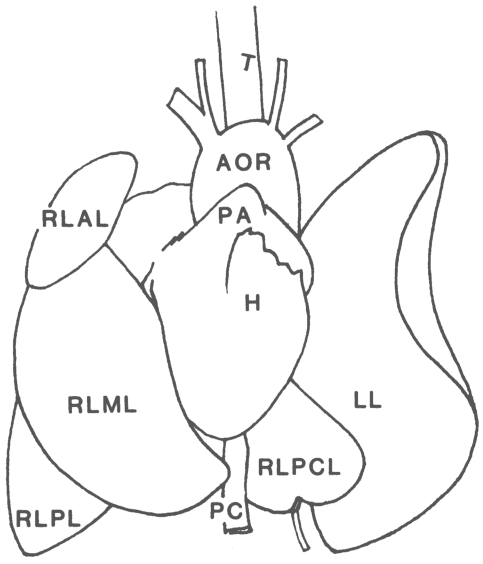

FIG. 5. A schematic of the white rat thoracic anatomy as modified from ref. 22. The mouse anatomy, although on a smaller scale, is similar. Abbreviations: aorta, AOR; heart, H; left lung, LL; pulmonary artery, PA; post cava, PC; right lung anterior lobe, RLAL; right lung middle lobe, RLML; right lung post caval lobe, RLPCL; right lung posterior lobe, RLPL; trachea, T.

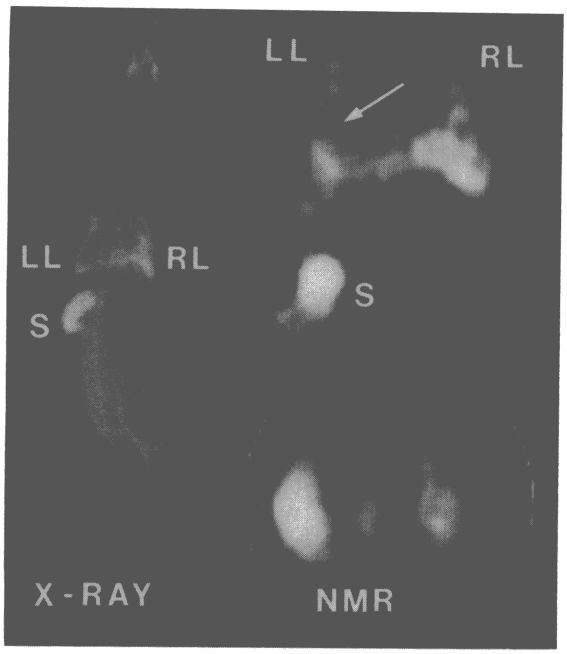

FIG. 7. Radiograph (posteroanterior) **(left)** and MR images **(right)** for a 2-to-1 mixture of FC-75/PFOB. A surgical procedure had produced an obstruction in one bronchial branch of the mouse prior to the liquid breathing. The arrow indicates the affected region on the coronal MR image. This was the only mouse that was not alive during the MR imaging experiments. Abbreviations: left lung, LL; right lung, RL; stomach, S. MR technique: 26.5 MHz (~0.66 T); partial saturation, TR 250 ms; 32 averages/projection; 72 projections.

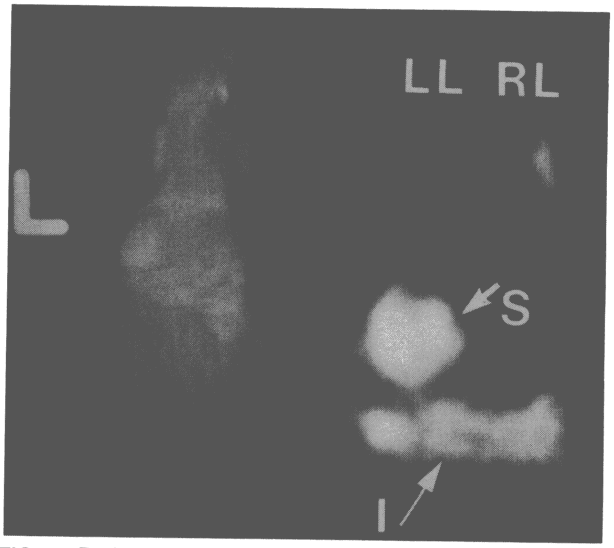

FIG. 8. Radiograph **(left)** and MR image **(right)** for a 9-to-1 mixture of FC-75/PFOB. A significant quantity of the perfluorocarbon compound (PFC) mixture had been swallowed by the mouse during the liquid breathing procedure. This figure illustrates the potential use of PFCs as gastrointestinal contrast agents. Abbreviations: intestines, I; left lung, LL; right lung, RL; stomach, S. MR technique: 26.5 MHz (~0.66 T); partial saturation, TR 500 ms; 32 averages/projection; 72 projections; gradient strength 0.1 G/cm.

quently, the MR images shown are those of the dead animal. (All other images shown in this paper are of living animals under self-sustained breathing.) Although the coronal MR image S/N is not high, there is an indication of a lack of PFC ventilation (arrow), which may represent an atelectatic region resulting from the induced defect. In the transverse image the left lung region is artificially enhanced due to the position of the animal in the RF coil, which allowed the stomach to be included within the nonslice selected transverse plane.

The final image set involving the FC-75/PFOB mixture (here in a ratio of 9-to-1, respectively) at 0.66 T is shown in Fig. 8. In this case the mouse appeared to have swallowed a significant amount of the PFC mixture with relatively little being introduced into the lungs. The radiograph and coronal MR images are presented primarily as further indication of the potential use of PFCs as ultra-high-contrast gastrointestinal contrast agents.

Figures 9 and 10 present FC-47 coronal and transverse images of two mice at 0.66 T under ambient air and pure oxygen breathing conditions. The signal strength enhancement provided by the pure oxygen environment was $\sim 1.75 \pm 0.15 \times$.

The next two figures show the MR images obtained on the low field system. Figure 11 includes a slice selective, 4 mm thick coronal proton image through the heart/lung region of a mouse following liquid breathing of APF-215 along with the corresponding nonslice selective coronal ^{19}F image taken immediately subsequent to the proton image. Close inspection of the two images reveals that the anatomical correlation between them is good. The proton image, although ungated, shows evidence of the myocardial wall with the heart positioned slightly toward the left. The associated heart shadow is apparent in the APF-215 image with the bright signal regions representing the PFC ventilated areas of the lungs corresponding on a 1-for-1 basis with the dark regions of the lung field on the proton image.

The APF-215 coronal lung images of another rat taken at 0.14 T are shown in Fig. 12. The enhancement in signal strength as a result of breathing pure oxygen versus ambient air was ~40%. This moderate increase is sufficient to improve visualization of lung field extent and general ventilation pattern.

SUMMARY AND CONCLUSIONS

These investigations demonstrate the potential use of PFCs as high contrast lung imaging agents. The fluorine image in correlation with the corresponding proton image would provide diagnostic in-

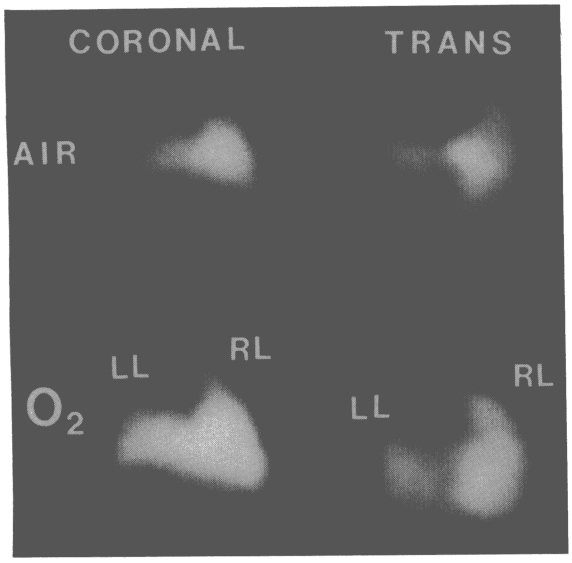

FIG. 9. Coronal **(left)** and transverse **(right)** FC-43 MR images of a mouse breathing ambient air and pure oxygen. An enhancement of ~1.6 to 1.9 × in image signal strength was observed when breathing pure oxygen. Abbreviations: left lung, LL; right lung, RL. MR technique: 26.5 MHz (~0.66 T); partial saturation, TR 250 ms; 32 averages/projection; 72 projections; gradient strength 0.1 G/cm.

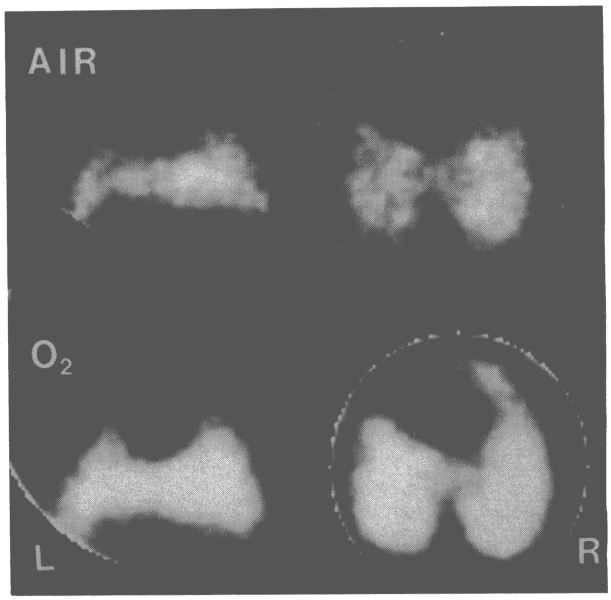

FIG. 10. Coronal **(left)** and transverse **(right)** FC-43 MR images of another mouse breathing ambient air and pure oxygen. An enhancement of ~1.7 to 1.9 × in image signal strength was observed when breathing pure oxygen. MR technique: 26.5 MHz (~0.66 T); partial saturation, TR 250 ms; averages/projection—coronal 32; transverse 64; 72 projections; gradient strength 0.18 G/cm.

formation concerning pulmonary ventilation performance in direct relationship to the specific anatomical condition. The clinical utility is advanced further through the possibility of obtaining quantitative regional P_{O_2} determination through calibrated T1 analysis. Multiple techniques would be available for introducing the PFCs into the pulmonary system including possibly aerosol spray and direct tracheal injection as well as liquid breathing for suitable situations. Shaffer et al. have published reports on the breathing of fluorocarbon liquids as a means of respiring newborn animals (23,24). Respiration with liquid fluorocarbons should find clinical application. It may be envisioned that ^{19}F MR imaging of the lung surfaces may be useful in diagnosing a variety of lung diseases (including ventilation defects and pulmonary carcinoma), in monitoring neonatal lung mechanics, and in possibly devising new treatments for cystic fibrosis and pulmonary emphysema.

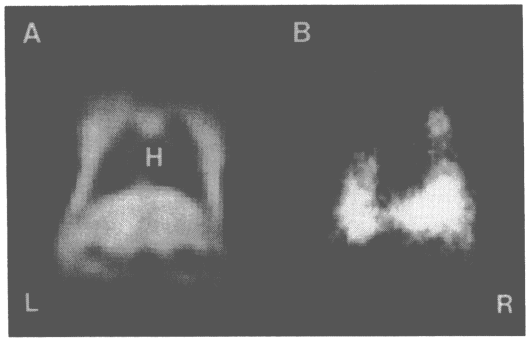

FIG. 11. a: The coronal proton image through the thorax of a rat. The lung field is demarcated as a low signal area. Although ungated, the heart wall (H) is visible. MR technique: 6.0 MHz (0.14 T for protons); 2DFT; TE 34 ms; TR 500 ms; 8 averages/phase amplitude; 64 phase amplitudes; gradient strength—0.06 G/cm. **b:** The coronal ^{19}F image of APF-215 in the same rat lungs taken sequentially immediately following (a). MR technique: 5.7 MHz (0.14 T for fluorine); partial saturation; TR 500 ms; 64 averages/projection; 72 projections; gradient strength 0.06 G/cm.

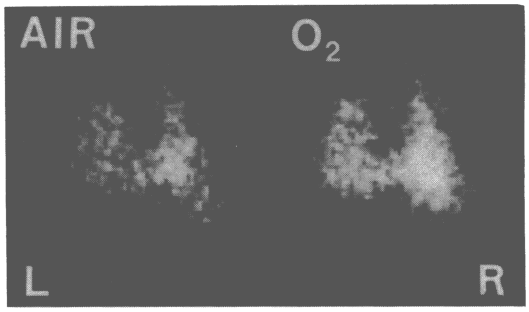

FIG. 12. Coronal images of APF-215 in the lungs of another rat under conditions of ambient air and pure oxygen breathing. An enhancement of ~40% in image signal strength was obtained when breathing pure oxygen. MR technique: 5.7 MHz (0.14 T); partial saturation; TR 250 ms; 64 averages/projection; 72 projections; gradient strength 0.04 G/cm.

Acknowledgments: This work was supported in part by grants from the National Institutes of Health HL 30104, 2-S07-RR07075, and 1 S10 RR01714 and from the National Science Foundation CHE-8102974. The assistance of Dr. Mariano Fernandez-Ulloa in performing the surgical procedure on the mouse of Fig. 7 is gratefully acknowledged.

REFERENCES

1. Clark LC Jr, Gollan F. Survival of mammals breathing organic liquids equilibrated with oxygen at atmospheric pressure. *Science* 1966;152:1755–6.
2. Wessler EP, Iltis R, Clark LC Jr. The solubility of oxygen in highly fluorinated liquids. *J Fluor Chem* 1977;9:137–46.
3. Clark LC Jr, Becattini F, Kaplan S, et al. Perfluorocarbons having a short dwell time in the liver. *Science* 1973;181: 680–2.
4. Ohyanagi H, Toshima K, Sekita M, et al. Clinical studies of perfluorochemical whole blood substitutes: safety of Fluosol-DA (20%) in normal human volunteers. *Clin Ther* 1979;2:306–12.
5. LeBlanc M, Riess JG. Artificial blood substitutes based on perfluorochemicals. In: Banks RE, ed. *Preparation, properties, and industrial applications of organic fluorine compounds*. London: Ellis Horwood, 1982:83–138.
6. *Perfluorochemical oxygen transport. International anesthesiology clinics, vol 23*. Boston: Little, Brown, 1985.
7. Holland GN, Bottomley PA, Hinshaw WS. ^{19}F magnetic resonance imaging. *J Magn Reson* 1977;28:133–6.
8. Heidelberger E, Lauterbur PD. Gas phase ^{19}F-NMR Zeugmatography: a new approach to lung ventilation imaging. In: *Society of Magnetic Resonance in Medicine first annual meeting program and book of abstracts*. Berkeley, CA: Society of Magnetic Resonance in Medicine, 1982: 70–1.
9. Thomas SR, Ackerman JL, Goebel BS, Davis M, Kereiakes JG, Lin Y-Y. Nuclear magnetic resonance imaging techniques as developed modestly within a university medical center environment: what can the small system contribute at this point? *Magn Reson Imag* 1982;1:11–21.
10. Clark LC Jr, Ackerman JL, Thomas SR, Millard RW. High contrast tissue and blood oxygen imaging based on fluorocarbon ^{19}F NMR relaxation times. *Abs J Magn Reson Med* 1984;1:135–6.
11. Clark LC Jr, Ackerman JL, Thomas SR. Perfluorinated organic liquids and emulsions as biocompatible NMR imaging agents for 19-F and dissolved oxygen. In: Bruley D, Bicher HI, Reneau D, eds. *Oxygen transport to tissue*. New York: Plenum, 1985. (Advances in medicine and biology; vol 6).
12. McFarland E, Koutcher JA, Rosen BR, Teicher B, Brady TJ. In vivo ^{19}F NMR imaging. *J Comput Assist Tomogr* 1985;9:8–15.
13. Lai CS, Stair SJ, Miziorko H, Hyde JS. Effect of oxygen and the lipid spin label TEMPO-laurate on fluorine-19 and proton relaxation rates of the perfluorochemical blood substitute, FC-43 emulsion. *J Magn Reson* 1984;57:447–52.
14. Thomas SR, Clark LC Jr, Ackerman JL, et al. NMR imaging of the lung using liquid perfluorocarbon. In: *Society of Magnetic Resonance in Medicine Third Annual Meeting, Abstracts*. Berkeley, CA: Society of Magnetic Resonance in Medicine: 1984.
15. Polak M, Navon G. Nuclear magnetic resonance studies of the interaction of molecular oxygen with organic compounds. *J Phys Chem* 1974;78:1747–50.
16. Delpuech JJ, Hamza MA, Serratrice G. Determination of oxygen by a nuclear magnetic resonance method. *J Magn Reson* 1979;36:173.
17. Hamza MA, Serratrice G, Stébé MJ, Delpuech JJ. Fluorocarbons as oxygen carriers. II. An NMR study of partially or totally fluorinated alkanes and alkenes. *J Magn Reson* 1981;42:227–41.
18. Parhami P, Fung BM. Fluorine-19 relaxation study of perfluorochemicals as oxygen carriers. *J Chem Phys* 1983;87:1928–31.
19. Kong CF, Holloway GM, Parhami P, Fung BM. Carbon-13 and fluorine-19 NMR study of perfluoro chemical emulsions. *J Phys Chem* 1984;88:6308–11.
20. Thomas SR, Ackerman JL, Kereiakes JG. Practical aspects involved in the design and set up of a 0.15 T, 6-coil resistive magnet, whole body NMR imaging facility. *Magn Reson Imag* 1984;2:341–8.
21. Busse LJ, Thomas SR, Pratt RG, Clark LC, Jr, Ackerman JL, Samaratunga RC. Deconvolution techniques for removing the effects of chemical shift in NMR imaging of perfluorocarbon compounds [Abstract]. *Med Phys* 1985;12:516.
22. Chiasson RB. *Laboratory anatomy of the white rat*. 2nd ed. Dubuque, IA: Wm. C. Brown, 1970.
23. Shaffer TH, Douglas PR, Lowe CA, Bhutani VK. The effects of liquid ventilation on cardiopulmonary function in preterm lambs. *Pediatr Res* 1983;17:303–6.
24. Shaffer TH, Tran N, Bhutani VK, Sivieri EM. Cardiopulmonary function in very preterm lambs during liquid ventilation. *Pediatr Res* 1983;17:680–4.